IMAGING HETEROGENEITY IN REGOLITH USING A JOINT GROUND PENETRATING RADAR AND SEISMOLOGY APPROACH. L. Wike[1] and J. Coonan[2], D. Kim[1,3], R. Ghent[4], S. Kruse[2], V. Lekic[1], J. Richardson[5], N. Schmerr[1], [1]lwike@umd.edu, University of Maryland, College Park, Department of Geology, 8000 Regents Dr. College Park, MD, USA 20742, [2]jcoonan@usf.edu, University of South Florida, Tampa, FL, [3]Institute of Geophysics, Zurich, Switzerland, [4]Planetary Science Institute, Tucson, AZ, [5]Goddard Space Flight Center, Greenbelt, MD.

Introduction: Radar and seismic techniques can provide information about the character of a planetary regolith. Here, we present preliminary results of our effort to synergistically employ spatially coincident shallow seismic and ground penetrating radar (GPR) techniques to gain quantitative information about the physical properties of the lunar regolith. We seek to use these complementary techniques in concert in order to reduce ambiguity in recovery of important physical regolith properties, particularly when little or no *a priori* ground truth information is available. Here, we report on numerical simulations of seismic and electromagnetic wave propagation through a common set of model spaces. Our goal is to use these simulations to validate methods, and determine optimal acquisition geometries for joint analysis of regolith containing voids, suspended rocks, or other scatterers.

Radar and seismic signals are scattered from wavelength-scale rocks, cracks, and other density discontinuities within the lunar regolith, though the relative strength of the scattering differs depending on the physical nature of the scatterers. At certain frequencies (e.g., at 50-200 Hz for seismic and 100-400 MHz for radar), radar and seismic scattering scale lengths (~meters) coincide, and so can provide complementary information. Various techniques have been used to invert these observed signals for information about the population of subsurface scatterers [e.g., 1-7], but it is often difficult to obtain a sufficiently detailed picture of, e.g., the subsurface rock population, to aid in landing site safety evaluation or to determine the exact depth to a subsurface feature of interest. Here, we seek to address this gap by quantifying the physical properties of the regolith using simultaneous analysis from coincident seismic and GPR arrays, taking advantage of the opposite effects of density contrasts on the respective elastic and electromagnetic wave speeds.

Joint Modeling Approach: We model the effects of regolith structure by simulating a void using both seismic and GPR modeling software. To start, we demonstrate the methodology using a single void: a semicircle of 25m radius, with its ceiling located at 25m depth. This void structure is placed within a basaltic composition matrix: a 300m by 100m prism for the seismic approach and a 130m by 90m prism for the GPR approach. We propagate simulated electromagnetic and seismic waves through the models containing the basaltic medium and vacuum-filled void, compute CMP-stacks, and migrate both records.

Ground Penetrating Radar. We use *gprMax* [8], a Finite-Difference-Time-Domain (FDTD) GPR modeling software, to construct the model space (Fig. 1a) and run the simulation. We use cell dimensions of 0.1m x 0.1m to allow for discretization of >10 cells per wavelength at a center frequency of 30 MHz. We use an array of 48 antennas placed 0.5m above the surface and at 2.5m spacing horizontally, with one serving as a source and the rest as receivers. We run the model 25 times, with the location of the source antenna being moved two array elements (5m) forward from its previous position for each run. We add 5m of space on the array edges to prevent boundary interactions.

The simulation outputs are converted to SEG2 format [9] for import into the *REFLEXW* software. We organize the individual shots (Fig. 1b) into a CMP gather, manually construct a 2D velocity profile using semblance analysis, stack the velocity profile (Fig. 1c) and perform a 2D Kirchhoff migration (Fig. 1d).

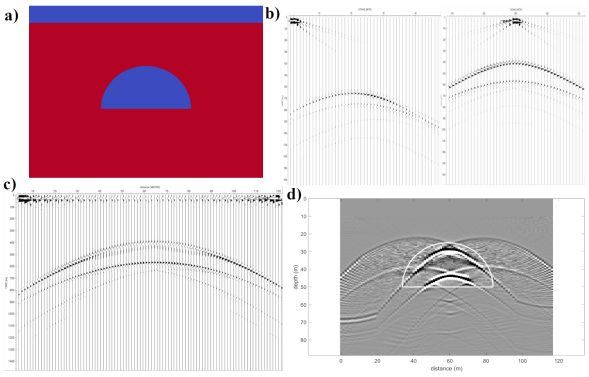

Fig. 1 a) *gprMax* model space. b) Individual shots from the leftmost antenna (left) and from directly above the center of the void (right). c) CMP stack from gather using 2D velocity model. d) Migration of the CMP stack with void geometry superimposed.

Reflected and Refracted Seismic Waves. We use the meshing software, *gmsh* [10], to create 9-node mesh spaces with physical properties calculated at node intersections. We convert our meshes to *SPECFEM2D*'s [11] format, and define the velocity and density of the void (orange) and basaltic

composition matrix (green) (Fig. 2a). *SPECFEM2D* computes the seismic wavefield given an at-surface moment tensor source with corner frequency of 100Hz, with simulation time spans of 100s of milliseconds. Thirteen single shots represent the source locations from 90m to 150m at the surface, spaced 5m apart, with the final source directly above the void. We simulate the wavefields of the geometry both with and without the void structure and difference the two, these differential waveforms show the reflected arrivals from the void (Fig. 2b).

We implemented CMP stacking (Fig. 2c) and 2D Kirchhoff migration (Fig. 2d) using the *CREWES MATLAB Software Library* [12] to image the void boundaries. The migrated image captures the depth and position of the void space, but has smearing near the vertical-most edges of the void. Some contamination comes from multiple reflections of the P-wave and S-wave from the top of the void; we do not resolve the void floor with this approach. This workflow will be applied to image subsurface structures in data from the Moon and terrestrial analog environments.

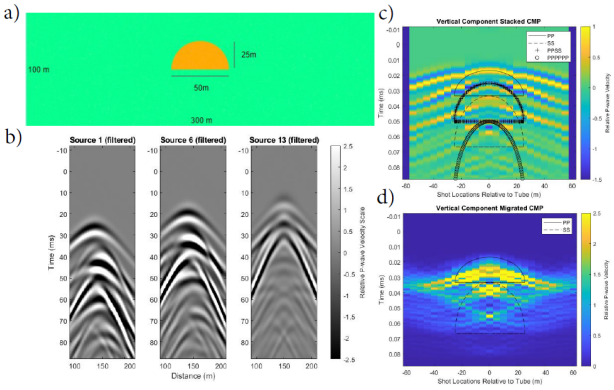

Fig. 2 a) *gmsh* model space. b) Velocity spectra of the synthetic wavefield generated by SPECFEM2D with void-induced hyperbolae. c) CMP stack of simulations for seismic sources 1-13 with PvP and SvS reflections corresponding to individual reflectors identified. d) Migration of the CMP stack to resolve void curvature.

Quantifying Heterogeneity: We quantitatively assess how random heterogeneities (scatterers) within the regolith affect the GPR and seismic waveforms and their joint inversions, using stochastic von Karman scattering media (Fig. 3). The media are defined by four parameters: Hurst exponent, a correlation length, an amplitude of seismic velocity variations, and an anisotropic scale. This allows us to generate realistic stochastic media, and explore the effects of sub-wavelength heterogeneity on the propagation of both GPR and seismic waves. We then assess to what extent frequency-dependent polarization analysis and filtering can help separate reflections from target structures from arrivals randomly scattered by the stochastic medium under various scenarios.

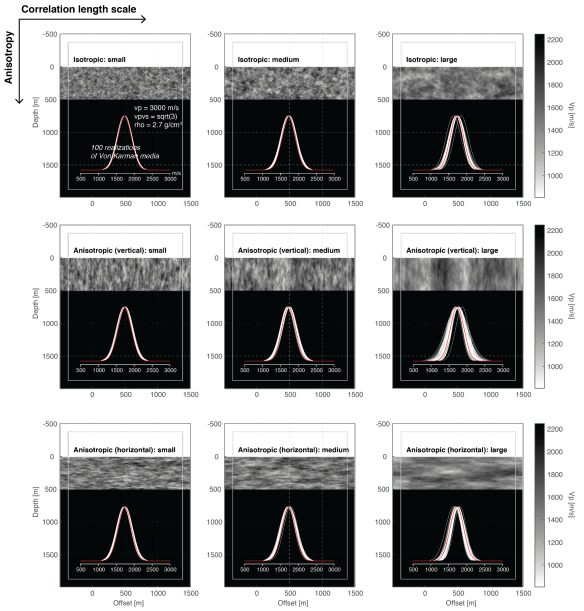

Fig. 3 Synthetic input velocity structures with a suite of random scattering media. Nine model cases (isotropic vs. anisotropic scattering media of varying correlation lengths) are built and we generate 100 random realizations of the scattering media for each.

Future directions: We will apply our seismic and GPR codes to in-situ field data. GEODES' seismic and GPR joint inversion project has an end goal of determining cost- and time-effective methods of finding and utilizing void spaces in new geophysics missions to the surfaces of Moon, asteroids, and Mars.

Acknowledgments: Funding for this project was supported by the NASA SSERVI GEODES grant 80NSSC19M0216.

References: [1]Xiao, L. et al. (2015) *Science, 347(6)*, 1226–1229. [2]Zhang, J. et al. (2015) *PNAS, 112(17),* 5342–5347. [3]Dainty, A. M., and M. N. Toksoz (1977) *J Geophys-Z Geophys, 43(1-2),* 375-388. [4]Blanchette-Guertin, J. F., et al. (2012) *JGR:Planets,117(E6)*,E06003. [5]Blanchette-Guertin, J. F. et al. (2015) *JGR-Planets, 120(3),* 515-537. [6]Watkins, J. S., and R. L. Kovach (1972) *Science, 175(4027),* 1244-1245. [7]Nakamura, Y., G. et al. (1982) *JGR, 87*, A117-A123.[8] Warren, C., et al. (2016) *Computer Phys. Comms 209,* 163-170. [9] Pullan, S. E. (1990) *Geophysics*, *55(9)*, 1260-1271.[10] Geuzaine C. and Remacle J.-F. (2009). *INT J NUMER METH ENG, 79, 11,* 1309-1331.[11]Tromp, J. et al. (2008). *CiCP, 3, 1*, 1-32.[12]Margrave, G.F., and Lamoureux, M.P. (2019). *Cambridge University Press*.